# STATE ESTIMATION BASED ON STOCHASTIC AND ZONOTOPIC APPROACHES: PART I - LINEAR SYSTEMS

Alesi Augusto de Paula*, Guilherme Vianna Raffo*, Bruno Otávio Soares Teixeira*

*Graduate Program in Electrical Engineering, Universidade Federal de Minas Gerais
Av. Antônio Carlos 6627, 31270-901, Belo Horizonte, MG, Brazil

Emails: alesi@ufmg.br, raffo@ufmg.br, brunoot@ufmg.br

**Resumo**— Este artigo revisa de forma comparativa os métodos de filtragem estocástica e zonotópica mais usuais na literatura para estimação de estados de sistemas lineares incertos. A média e o nível de confiança da variável aleatória Gaussiana são comparados com o centro e a incerteza da variável zonotópica. Para isso, uma notação unificada para estas abordagens é proposta. Por um lado, o filtro de Kalman é um algoritmo muito utilizado por tratar estados como variáveis Gaussianas, cuja função distribuição de probabilidade é de simples representação. Por outro lado, a estimação de estados zonotópicos tem ganhado relevância na literatura por causa de propriedades intrínsecas a conjuntos, que garantem inclusão dos estados exatos nos conjuntos estimados e ganho computacional no cômputo de domínios.

**Palavras-chave**— Filtro de Kalman, filtro zonotópico, estimação de estados, sistemas lineares.

**Abstract**— This paper presents a comparative review on the most usual stochastic and zonotopic filtering methods in the literature for state estimation of uncertain linear systems. The mean and the confidence level of the Gaussian random variable are compared to the center and uncertainty of the zonotopic variable. To achieve that, a unified notation for these approaches is proposed. On one hand, the Kalman filter is an algorithm often used for treating states as Gaussian variables, whose probability density function is simple to represent. On other hand, the estimation of zonotopic states has owned relevance in the literature due to intrinsic properties of sets, which guarantee inclusion of the exact states into the estimated sets and improved computational burden on the computation of domains.

**Keywords**— Kalman filter, zonotopic filter, state estimation, linear systems.

## 1 Introduction

Since 1960, based on the well-known Kalman filter (KF) (Kalman et al., 1960), state estimation has reached important role in the literature. The KF minimizes the variance of the state estimate of a given linear process based on the Kalman gain. Assuming Gaussian noise terms present in a linear system, the KF is optimal in the perspectives of mean, likelihood and mode (Gelb, 1974; Jazwinski, 2007). However, assumptions of noise distributions may be hard to verify in practice, mainly due to the Gaussian variable unlimited support.

There are many ways to represent states of a given process. The usual KF treats each state as a random variable (RV) using statistical concepts (Kay, 1993). States can also be represented by sets using interval arithmetic (Moore et al., 2009) and affine arithmetic (Le et al., 2013), which generate convex sets by affine transformations of intervals. Affine transformation is a more general way to represent compact and convex sets.

Over the last two decades, the set membership theory has owned relevance in the literature. The main motivation to use sets in state estimation is to consider that the noise terms in a given system are unknown but bounded (Alamo et al., 2005). In this case, uncertainty is represented by the set approach rather than the stochastic one. Zonotopes are special cases of convex polytopes, which are compact and centrally symmetric sets (Le et al., 2013). Many researches have been conducted using zonotopes, due to the proprieties of sum of two zonotopes and affine transformations, which guarantee reduction of computational burden when computing domains. Moreover, as all set membership technique, zonotopes guarantee true states belong to the estimated set under some hypothesis.

In 2005, the zonotopic filter (ZF) was proposed by Alamo et al. (2005). This algorithm is based on zonotopes and presents similar steps to the KF, namely: *forecast* and *data-assimilation.* In this last step, an intersection is performed to obtain a zonotope, which can be computed by two different criteria: segment minimization and volume minimization. The first one is the fastest computationally, while the other one leads to the smallest intersection volume and spends much more time due to an optimization algorithm being executed. In (Bravo et al., 2006), the volume minimization approach is reformulated to let the ZF be much faster.

In (de Almeida Neto et al., 2014), a comparison between the KF and the ZF is presented based on numerical results for a specific case study. Basically, these filters are used as alternatives to estimate the position of unmanned air vehicles while the GPS does not yield new measurements. According to the numerical results, the used ZF with the segment minimization, led to larger uncertainty than the KF did.

In this paper, the stochastic and zonotopic approaches are compared for the state estimation of linear systems by means of KF (Kalman et al., 1960) and ZF (Alamo et al., 2005). Theses filters are presented for the non-autonomous case and they aim reducing uncertainty, since the KF is a minimum-variance estimator and the ZF is used with the volume minimization criterion. This paper is a generalization of (de Almeida Neto et al., 2014), since it presents: (i) a general way to estimate states of any linear system; (ii) main advantages related to each approach; and (iii) the ZF with two minimization approaches, namely, segment minimization (Alamo et al., 2005) and the improved volume minimization criterion (Bravo et al., 2006). Since the core of the methods is in the transformations of uncertain variables, the results of affine transformations related to each approach are also presented. Furthermore, a unified notation is proposed to the filters, in order to explicit their similarities.

This paper is organized as follows. Section 2 presents some concepts and results of the affine transformation of a Gaussian random variable (GRV) and a zonotopic variable (ZV). Section 3 formulates the problem under investigation. In Section 4, the algorithms KF and ZF are presented. In the Section 5, these algorithms are applied to an illustrative example. Finally, conclusions are presented in Section 6.

## 2 Background

Preliminary basic definitions and notations are introduced to characterize both GRV, according to statistical concepts, and ZV using interval arithmetic.

### *2.1 Random Variables*

RV is a function that maps a sample space $\mathbb{S}$ in the set of real numbers $\mathbb{R}^n$ (Kay, 1993). A random variable $X$ is described by a probability density function (PDF) $p(x)$, where $x$ is a realization of $X$, such that $x \in X$. The *mean* $\hat{x}$ of the RV $X$ is defined as

$$\hat{x} = \mathrm{E}[X] \triangleq \begin{bmatrix} \int_{-\infty}^{+\infty} x_1 p(x_1) dx_1 \\ \int_{-\infty}^{+\infty} x_2 p(x_2) dx_2 \\ \vdots \\ \int_{-\infty}^{+\infty} x_n p(x_n) dx_n \end{bmatrix} = \begin{bmatrix} \hat{x}_1 \\ \hat{x}_2 \\ \vdots \\ \hat{x}_n \end{bmatrix},$$

where $\mathrm{E}[\bullet]$ is the *expected value* operator. The *covariance matrix* $P^{\mathrm{xx}}$ of a RV $X$ is defined as

$$P^{\mathrm{xx}} = \mathrm{cov}(X) \triangleq \int_{-\infty}^{+\infty} (x-\hat{x})(x-\hat{x})^{\mathrm{T}} p(x) dx.$$

For brevity, in the case of a GRV $X$, its PDF is fully characterized by its mean $\hat{x}$ and covariance matrix $P^{\mathrm{xx}}$ as (Kay, 1993)

$$p(x) = \frac{\exp\left\{-\frac{1}{2}(x-\hat{x})^{\mathrm{T}} \left(P^{\mathrm{xx}}\right)^{-1} (x-\hat{x})\right\}}{(2\pi)^{n/2}\sqrt{\det\left(P^{\mathrm{xx}}\right)}}.$$

A GRV $X$ is represented by $X \sim \mathcal{N}(\hat{x}, P^{\mathrm{xx}})$.

### *2.2 Interval Arithmetic and Zonotopes*

*Set* is a grouping of elements with similar characteristics, like ellipsoids, polytopes, intervals and zonotopes. The interval $[x] \triangleq [\underline{x}; \overline{x}]$ is the set $\{x \in \mathbb{R} : \underline{x} \leq x \leq \overline{x}\}$. The unitary interval is denoted as $[\Phi] = [-1; 1]$. A box is a $n$-dimensional interval vector defined as

$$[x] \triangleq \{x \in \mathbb{R}^n : \underline{x}_i \leq x_i \leq \overline{x}_i,\ i = 1, 2, ..., n\}.$$

The unitary box composed by $n_g$ unitary intervals is denoted as $[\Phi]^{n_g}$. Given a box $[x]$, $\mathrm{mid}([x])_i \triangleq \dfrac{\underline{x}_i + \overline{x}_i}{2}$ is the $i$-th midpoint and $\mathrm{diam}([x])_i \triangleq \overline{x}_i - \underline{x}_i$ is the $i$-th diameter. The absolute value of the interval $[x]$ is given by $|[x]| \triangleq \max\{|\underline{x}|, |\overline{x}|\}$. The $\infty$-norm of the box $[x]$ is defined as $||[x]||_\infty \triangleq \max_i |[x_i]|$.

Consider two intervals $[x] = [\underline{x}; \overline{x}]$ and $[y] = [\underline{y}; \overline{y}]$. The four basic interval operations are given by (Moore et al., 2009)

$$\begin{aligned} [x] + [y] &\triangleq [\underline{x} + \underline{y}; \overline{x} + \overline{y}], \\ [x] - [y] &\triangleq [\underline{x} - \overline{y}; \overline{x} - \underline{y}], \\ [x] \cdot [y] &\triangleq [\min\{S\}; \max\{S\}], \\ [x]/[y] &\triangleq [x] \cdot \left[\frac{1}{\overline{y}}; \frac{1}{\underline{y}}\right], \text{ if } y \in \mathbb{R}_+, \end{aligned}$$

where $S = \{\underline{x}\underline{y}, \underline{x}\overline{y}, \overline{x}\underline{y}, \overline{x}\overline{y}\}$.

Therewith, it is possible to present the fundamental theorem of the interval arithmetic.

**Theorem 2.1** *Natural interval extension (Alamo et al., 2005). Let $y = h(x)$ be a general nonlinear transformation, where $h : \mathbb{R}^n \to \mathbb{R}^m$ is a standard continuous function. Given an interval $[x] \in \mathbb{R}^n$, the natural interval extension $\triangle\{h\}$ is obtained substituting $x$ by $[x]$ and all standard operations by corresponding interval operations, such that $h([x]) \subseteq \triangle\{h\}([x])$, where $h([x])$ is the exact transformation of the interval $[x]$.*

**Definition 2.1** *Minkowski sum (Alamo et al., 2005). The Minkowski sum of two sets is defined by*

$$\mathcal{X} \oplus \mathcal{Y} \triangleq \{x + y : x \in \mathcal{X}, y \in \mathcal{Y}\},$$

*which corresponds to the point-to-point sum.*

**Definition 2.2** *Zonotope (Alamo et al., 2005). Given a vector $\hat{x} \in \mathbb{R}^n$ and a matrix $G^{\mathrm{x}} \in \mathbb{R}^{n \times n_g}$, a zonotope $\mathcal{X}$ of order $n_g$ is defined as*

$$\hat{x} \oplus G^{\mathrm{x}}[\Phi]^{n_g} = \{\hat{x} + G^{\mathrm{x}}\xi : \xi \in [\Phi]^{n_g}, ||\xi||_\infty \leq 1\},$$

*where $\hat{x}$ and $G^{\mathrm{x}}$ are the center and generator matrix of the zonotope $\mathcal{X}$, respectively, and $||\bullet||_\infty$ is the $\infty$-norm of a vector.*

Thus, a ZV $\mathcal{X}$ is a variable whose values satisfy $x \in \mathcal{X}$. Furthermore, note that zonotope is a affine transformation of the unitary box $[\Phi]^{n_g}$.

A width measure of zonotope can be given by the *Frobenius norm*, which is based on the 2-norm of each generator segment, that is, the column of the generator matrix $G^{\mathrm{x}}$.

**Definition 2.3** *Let $G^{\mathrm{x}}$ be the generator matrix of a zonotope such that $G^{\mathrm{x}} = \begin{bmatrix} g_1^{\mathrm{x}} & g_2^{\mathrm{x}} & \dots & g_{n_g}^{\mathrm{x}} \cdot \end{bmatrix}$ The Frobenius norm of the generator matrix is defined as*

$$||G^{\mathrm{x}}||_{\mathrm{F}} \triangleq \sqrt{\sum_{j=1}^{n_g} ||g_j^{\mathrm{x}}||_2^2}, \tag{1}$$

*where $||\bullet||_2$ is the 2-norm of a matrix.*

### *2.3 Affine Transformations*

This section presents the results of affine transformations of both GRV and ZV. Let

$$Y = AX + b \tag{2}$$

be an affine transformation of the prior variable $X$. The two following results show how a GRV and a ZV propagate through an affine transformation.

**Fact 2.1** *Let $X \sim \mathcal{N}(\hat{x}, P^{\mathrm{xx}})$ be a GRV. Applying the affine transformation $Y = AX + b$ generates another GRV $Y \sim \mathcal{N}(\hat{y}, P^{\mathrm{yy}})$, where*

$$\hat{y} = A\hat{x} + b, \tag{3}$$
$$P^{\mathrm{yy}} = AP^{\mathrm{xx}}A^{\mathrm{T}}. \tag{4}$$

**Fact 2.2** *Let $\mathcal{X} = \hat{x} \oplus G^{\mathrm{x}}[\Phi]^{n_g}$ be a ZV, where $\hat{x}$ and $G^{\mathrm{x}}$ are the center and generator matrix, respectively. Applying the affine transformation $\mathcal{Y} = A\mathcal{X} \oplus b$ generates another ZV $\mathcal{Y} = \hat{y} \oplus G^{\mathrm{y}}[\Phi]^{n_g}$, where*

$$\hat{y} = A\hat{x} + b, \tag{5}$$
$$G^{\mathrm{y}} = AG^{\mathrm{x}}. \tag{6}$$

Note that the uncertainties of the variables $X$ and $\mathcal{X}$ are related to the covariance matrix $P^{\mathrm{xx}}$ and the generator matrix $G^{\mathrm{x}}$. According to Facts 2.1 and 2.2, the transformed variables $Y$ and $\mathcal{Y}$ can be more uncertain or less uncertain than the input variables, $X$ and $\mathcal{X}$, according to the matrix $A$.

### *2.4 Order Reduction*

It is common to reduce the order $n_g$ of a zonotope $\mathcal{X}$ in order $\varphi$ to obtain other one $\downarrow_\varphi \mathcal{X}$, but with the same center $\hat{x}$. This new zonotope is more conservative than the former, but it reduces the computational burden over operations. Given the desired order $\varphi$, the order reduction algorithm of a zonotope $\mathcal{X}$ is presented next.

**Algorithm 2.1** *Zonotope order reduction (Combastel, 2005).*
*1: Procedure $\downarrow_\varphi G^{\mathrm{x}} = \mathrm{red\_order}(G^{\mathrm{x}}, \varphi)$.*
*2: Calculate the 2-norm of each generator $g_j^{\mathrm{x}} = \mathrm{col}_j(G^{\mathrm{x}}) \in \mathbb{R}^n$ of the matrix $G^{\mathrm{x}}$ and sort them in descending order:*

$$G^{\mathrm{xs}} = \begin{bmatrix} g_1^{\mathrm{x}} & \cdots & g_j^{\mathrm{x}} & \cdots & g_{n_g}^{\mathrm{x}} \end{bmatrix}, \tag{7}$$

*where $||g_j^{\mathrm{x}}||_2 \geq ||g_{j+1}^{\mathrm{x}}||_2$.*
*3: If $n_g \leq \varphi$, then $\downarrow_\varphi G^{\mathrm{x}} = G^{\mathrm{xs}}$. Otherwise, given the sorted matrix $G^{\mathrm{xs}}$, determine the matrices*

$$G_>^{\mathrm{x}} = \begin{bmatrix} g_1^{\mathrm{x}} & \cdots & g_{\varphi-n}^{\mathrm{x}} \end{bmatrix}, \tag{8}$$

*which are the first $\varphi - n$ columns of $G^{\mathrm{xs}}$, and*

$$G_<^{\mathrm{x}} = \begin{bmatrix} g_{\varphi-n+1}^{\mathrm{x}} & \cdots & g_{n_g}^{\mathrm{x}} \end{bmatrix}, \tag{9}$$

*which are the remaining columns of $G^{\mathrm{xs}}$.*
*4: Calculate the matrix*

$$G^{\mathrm{b}} = \mathrm{diag}\left(|G_<^{\mathrm{x}}|\, 1_{n_{g<} \times 1}\right), \tag{10}$$

*where $|G_<^{\mathrm{x}}|$ is the absolute value of each element of the matrix $G_<^{\mathrm{x}}$, $1_{n_{g<} \times 1}$ is the vector of unitary elements, and $\mathrm{diag}(\bullet)$ is the returned diagonal matrix.*
*5: Finally, calculate the reduced generator matrix $\downarrow_\varphi G^{\mathrm{x}}$ given by*

$$\downarrow_\varphi G^{\mathrm{x}} = \begin{bmatrix} G_>^{\mathrm{x}} & G^{\mathrm{b}} \end{bmatrix}. \tag{11}$$

□

The following example is proposed to illustrate the affine transformations of a GRV and a ZV, as well as the operation of zonotope order reduction.

**Example 2.1** *Consider the transformation $y = Ax + b$, with $A = 1.5I_{2\times 2}$, $b = \begin{bmatrix} 0.5 & 0.5 \end{bmatrix}^{\mathrm{T}}$ and $I_{2\times 2} \in \mathbb{R}^2$ the identity matrix, the GRV $X \sim \mathcal{N}(1_{2\times 1}, I_{2\times 2})$ and the ZV $\mathcal{X} = \begin{bmatrix} 1 \\ 1 \end{bmatrix} \oplus \begin{bmatrix} 1 & 2 & 3 & 4 \\ 4 & 3 & 2 & 1 \end{bmatrix} [\Phi]^4$. In Figure 1, the PDF of $X$, the zonotopic set of $\mathcal{X}$ and the corresponding transformations are presented. Moreover, the order reduction of the zonotope $\mathcal{X}$ to $\downarrow_3 \mathcal{X}$, $\varphi = 3$, is illustrated.*

□

(a)

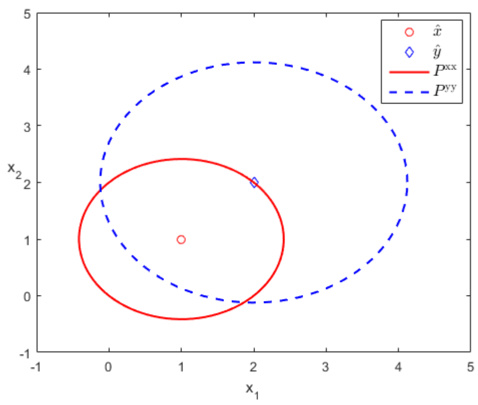


(b)

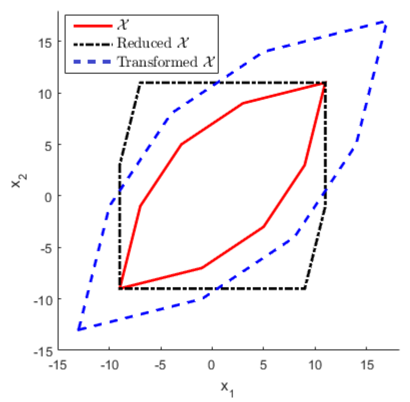


Figure 1: Graphic example of the affine transformation $y = Ax + b$, in blue dashed line, of: (a) a GRV $X$ and (b) a ZV $\mathcal{X}$ in red solid line. In (b), the zonotope $\mathcal{X}$ is presented after its reduction (black dash-dotted line) using $\varphi = 3$.

## 3 Problem Formulation

Consider the discrete-time linear dynamical system

$$x_k = A_{k-1}x_{k-1} + B_{k-1}u_{k-1} + B^{\mathrm{w}}_{k-1}w_{k-1}, \quad (12)$$
$$y_k = C_k x_k + D^{\mathrm{v}}_k v_k, \quad (13)$$

where $A_{k-1}$, $B_{k-1}$, $B^{\mathrm{w}}_{k-1}$, $C_k$ and $D^{\mathrm{v}}_k$ are time-varying matrices, $x_k \in \mathbb{R}^n$ is the state vector to be estimated, $u_{k-1}$ is the input vector, $y_k$ is the output vector, $w_k \in \mathbb{R}^q$ and $v_k \in \mathbb{R}^r$ are the process and measurement noise terms, respectively. The input vector $u_k$, the measurements $y_k$ and the matrices $A_{k-1}$, $B_{k-1}$, $B^{\mathrm{w}}_{k-1}$, $C_k$ and $D^{\mathrm{v}}_k$ are assumed to be known for $\forall k \geq 1$. Two different assumptions can be made on the noise terms.

In the stochastic approach, the noise terms are white, Gaussian and uncorrelated, with zero mean and covariance matrices $\mathrm{E}\left[w_k w_k^{\mathrm{T}}\right] = Q_k$ and $\mathrm{E}\left[v_k v_k^{\mathrm{T}}\right] = R_k$. The estimates of the initial state $\hat{x}_0$ with covariance $P^{\mathrm{xx}}_0$ and the covariance matrices $Q_{k-1}$ and $R_k$ are assumed to be known.

In the zonotopic approach, the noise terms are unknown but bounded by the corresponding zonotopes $w_{k-1} \in \mathcal{W}_{k-1}$ and $v_k \in \mathcal{V}_k$. The initial states must satisfy the zonotopic set $x_0 \in \mathcal{X}_0$. The sets $\mathcal{W}_{k-1} = \hat{w}_{k-1} \oplus G^{\mathrm{w}}_{k-1}[\Phi]^{n^{\mathrm{w}}_g}$, $\mathcal{V}_k = \hat{v}_k \oplus G^{\mathrm{v}}_k[\Phi]^{n^{\mathrm{v}}_g}$ and $\mathcal{X}_0 = \hat{x}_0 \oplus G^{\mathrm{x}}_0[\Phi]^{n^{\mathrm{x}}_g}$ are assumed to be known.

## 4 Linear State Estimators

The KF and the ZF basically propagate the initial GRV $X_{k-1}$ and ZV $\mathcal{X}_{k-1}$ by the process model (12) to obtain the *a priori* estimates $X_{k|k-1}$ and $\mathcal{X}_{k|k-1}$, respectively. After, their estimates are used to calculate the transformed variables $Y_{k|k-1}$ and $\mathcal{Y}_{k|k-1}$ using the measurement model (13). Finally, the information related to these two steps are weighted to obtain the *a posteriori* estimates $X_k$ and $\mathcal{X}_k$. The algorithms for each filter are presented in the following subsections based on two steps, namely: forecast and data-assimilation.

### 4.1 Kalman Filter

The forecast step is executed using the process model (12), and calculating the *a priori* estimates as $X_{k|k-1} \sim \mathcal{N}\left(\hat{x}_{k|k-1}, P^{\mathrm{xx}}_{k|k-1}\right)$, where

$$\hat{x}_{k|k-1} = A_{k-1}\hat{x}_{k-1} + B_{k-1}u_{k-1}, \quad (14)$$
$$P^{\mathrm{xx}}_{k|k-1} = A_{k-1}P^{\mathrm{xx}}_{k-1}A^{\mathrm{T}}_{k-1} + B^{\mathrm{w}}_{k-1}Q_{k-1}\left(B^{\mathrm{w}}_{k-1}\right)^{\mathrm{T}}. \quad (15)$$

Using the measurement model (13) and the prior estimates, calculate the estimates related to the transformed variable $Y_k \sim \mathcal{N}\left(\hat{y}_{k|k-1}, P^{\mathrm{yy}}_{k|k-1}\right)$ as

$$\hat{y}_{k|k-1} = C_k\hat{x}_{k|k-1}, \quad (16)$$
$$P^{\mathrm{xy}}_{k|k-1} = P^{\mathrm{xx}}_{k|k-1}C^{\mathrm{T}}_k, \quad (17)$$
$$P^{\mathrm{yy}}_{k|k-1} = C_k P^{\mathrm{xx}}_{k|k-1}C^{\mathrm{T}}_k + D^{\mathrm{v}}_k R_k\left(D^{\mathrm{v}}_k\right)^{\mathrm{T}}. \quad (18)$$
$$(19)$$

The data-assimilation step is performed by calculating the Kalman gain as

$$K_k = P^{\mathrm{xy}}_{k|k-1}\left(P^{\mathrm{yy}}_{k|k-1}\right)^{-1}, \quad (20)$$

and after, computing the properties of the *a posteriori* variable $X_k \sim \mathcal{N}\left(\hat{x}_k, P^{\mathrm{xx}}_k\right)$, where

$$\hat{x}_k = \hat{x}_{k|k-1} + K_k\left(y_k - \hat{y}_{k|k-1}\right), \quad (21)$$
$$P^{\mathrm{xx}}_k = P^{\mathrm{xx}}_{k|k-1} - K_k P^{\mathrm{yy}}_{k|k-1}K^{\mathrm{T}}_k. \quad (22)$$

### 4.2 Zonotopic Filter

This algorithm is presented for the non-autonomous case (Rego and Raffo, 2016) with two types of intersection, namely: segment minimization, proposed by Alamo et al. (2005), and improved volume minimization, proposed by Bravo et al. (2006). The ZF algorithm presents four steps: (i) prediction, (ii) measurement, (iii) intersection and (iv) order reduction, where (i) can be considered the forecast step while (ii)-(iv) constitute the data-assimilation step. In the first one, the ZF uses information related to the process model (12) to determine a predicted zonotope $\mathcal{X}_{k|k-1}$. After, this predicted zonotope, the measurement model (13) and the measurements $y_k$ are used to determine a strip $\mathcal{Y}_{k|k-1}$. In the intersection step, the final zonotope $\mathcal{X}_k$ incorporates information related to both system model and measurements through any minimization criterion. Finally, the latter zonotope is reduced based on the order $\varphi$.

At first, given the process model (12), the zonotope $\mathcal{X}_{k-1} = \hat{x}_{k-1} \oplus G^{\mathrm{x}}_{k-1}[\Phi]^{n^{\mathrm{x}}_g}_{k-1}$, and the zonotope $\mathcal{W}_{k-1} = \hat{w}_{k-1} \oplus G^{\mathrm{w}}_{k-1}[\Phi]^{n^{\mathrm{w}}_g}$, determine the predicted zonotope $\mathcal{X}_{k|k-1} = \hat{x}_{k|k-1} \oplus G^{\mathrm{x}}_{k|k-1}[\Phi]^{n^{\mathrm{x}}_g}_{k|k-1}$, where

$$\hat{x}_{k|k-1} = A_{k-1}\hat{x}_{k-1} + B_{k-1}u_{k-1} + B^{\mathrm{w}}_{k-1}\hat{w}_{k-1}, \tag{23}$$

$$G^{\mathrm{x}}_{k|k-1} = \begin{bmatrix} B^{\mathrm{w}}_{k-1}G^{\mathrm{w}}_{k-1} & A_{k-1}G^{\mathrm{x}}_{k-1} \end{bmatrix}. \tag{24}$$

Next, given the zonotope $\mathcal{V}_k = \hat{v}_k \oplus G^{\mathrm{v}}_k[\Phi]^{n^{\mathrm{v}}_g}$ and the measurement model (13), use interval arithmetic to obtain the box

$$[\Lambda] = \triangle\left\{D^{\mathrm{v}}_k \mathcal{V}_k\right\} \tag{25}$$

and the scalars

$$s_i = \mathrm{mid}([\Lambda]) \in \mathbb{R}, \tag{26}$$

$$\rho_i = \frac{1}{2}\mathrm{diam}([\Lambda]) \in \mathbb{R}. \tag{27}$$

Let $c_i \in \mathbb{R}^n$ be a vector defined by the $i$-th row of the matrix $C_k$, $c_i = \mathrm{row}_i\left(C_k\right)^{\mathrm{T}}$. Then, based on $c_i$, the $i$-th measurement $y_{i,k} \in \mathbb{R}$ and the scalars $s_i$ and $\rho_i$, a strip $\mathcal{Y}_{i,k|k-1} = \left\{x \in \mathbb{R}^n : \left|c_i^{\mathrm{T}}x - d_i\right| \leq \rho_i\right\}$ is defined, where $d_i = y_{i,k} + s_i$.

After, calculate the intersection $\mathcal{X}_k$ between the predicted zonotope $\mathcal{X}_{k|k-1} = \hat{x}_{k|k-1} \oplus \begin{bmatrix} g^{\mathrm{x}}_1 & g^{\mathrm{x}}_2 & \ldots & g^{\mathrm{x}}_{n_g}\end{bmatrix}[\Phi]^{n_g}$ and the strip $\mathcal{Y}_{k|k-1} = \left\{x \in \mathbb{R}^n : \left|c^{\mathrm{T}}x - d\right| \leq \rho\right\}$. Two different criteria are presented, namely: segment minimization and volume minimization. The first one minimizes the Frobenius norm of the generator matrix of the intersection $\mathcal{X}_k$. This criterion is used when it is necessary to reduce computational burden, mainly due to great order reduction $\varphi$. According to the predicted zonotope $\mathcal{X}_{k|k-1}$ and the strip $\mathcal{Y}_{k|k-1}$, compute the vector $\lambda \in \mathbb{R}^n$

$$\lambda = \frac{G^{\mathrm{x}}_{k|k-1}\left(G^{\mathrm{x}}_{k|k-1}\right)^{\mathrm{T}}c}{c^{\mathrm{T}}G^{\mathrm{x}}_{k|k-1}\left(G^{\mathrm{x}}_{k|k-1}\right)^{\mathrm{T}}c + \rho^2}. \tag{28}$$

Thus, the intersection $\mathcal{X}_k$ is given by

$$\hat{x}_k = \hat{x}_{k|k-1} + \lambda\left(d - c^{\mathrm{T}}\hat{x}_{k|k-1}\right), \tag{29}$$

$$G^{\mathrm{x}}_k = \begin{bmatrix}\left(I_{n\times n} - \lambda c^{\mathrm{T}}\right)G^{\mathrm{x}}_{k|k-1} & \rho\lambda\end{bmatrix}. \tag{30}$$

If there are more than one measurement, this zonotope is used to define another strip and a new intersection is performed with all of them, until all measurements $y_{i,k}$, $i = 1, ..., m$, are used.

Finally, given the desired order $\varphi$, use Algorithm 2.1 on the zonotope $\mathcal{X}_k$ to obtain $\downarrow_{\varphi} G^{\mathrm{x}}_k = \mathrm{red\_order}(G^{\mathrm{x}}_k, \varphi)$.

Alternatively, another criterion to compute the intersection $\mathcal{X}_k$ is to reduce its volume for $j = 0, 1, ..., n_g$. Then, $(n_g + 1)$ zonotopes $\bar{\mathcal{X}}(j) = \bar{x}(j) \oplus \bar{G}(j)[\Phi]^{n_g}$ are defined as the intersection between $\mathcal{X}_{k|k-1}$ and $\mathcal{Y}_{k|k-1}$, where

$$\bar{x}(j) = \begin{cases} \hat{x}_{k|k-1} + \frac{\left(d - c^{\mathrm{T}}\hat{x}_{k|k-1}\right)}{c^{\mathrm{T}}g^{\mathrm{x}}_j}g^{\mathrm{x}}_j, & \text{if } 1 \leq j \leq n_g \\ & \text{and } c^{\mathrm{T}}g^{\mathrm{x}}_j \neq 0 \\ \hat{x}_{k|k-1}, & \text{otherwise,} \end{cases} \tag{31}$$

$$\bar{g}^j_i = \begin{cases} g^{\mathrm{x}}_i - \frac{c^{\mathrm{T}}g^{\mathrm{x}}_i}{c^{\mathrm{T}}g^{\mathrm{x}}_j}g^{\mathrm{x}}_j, & \text{if } i \neq j \\ \frac{\rho}{c^{\mathrm{T}}g^{\mathrm{x}}_j}g^{\mathrm{x}}_j, & \text{if } i = j, \end{cases} \tag{32}$$

$$\bar{G}(j) = \begin{cases} \begin{bmatrix}\bar{g}^j_1 & \bar{g}^j_2 & \ldots & \bar{g}^j_{n_g}\end{bmatrix}, & \text{if } 1 \leq j \leq n_g \\ & \text{and } c^{\mathrm{T}}g^{\mathrm{x}}_j \neq 0 \\ G^{\mathrm{x}}, & \text{otherwise.} \end{cases} \tag{33}$$

The chosen zonotope is the one with the smallest volume based on the zonotope volume equation

$$\mathrm{Vol}\left(\bar{\mathcal{X}}\right) = 2^n \sum_{i=1}^{N(n_g,n)} \left|\det(T_i)\right|, \tag{34}$$

where $N\left(n_g, n\right)$ is the mathematical combination that returns all possible ways to choose $n$ elements of a set $n_g$, and $T_i \in \mathbb{R}^{n\times n}$ denotes all the matrices that can be obtained taking $n$ columns of the matrix $\bar{G}$.

## 5 Numerical Example

### *5.1 Process Description*

Consider the discrete-time linear dynamical system defined as (Alamo et al., 2005)

$$x_k = \begin{bmatrix} 0 & -0.5 \\ 1 & 1 + 0.3\zeta_{k-1}\end{bmatrix}x_{k-1} + 0.02\begin{bmatrix}-6 \\ 1\end{bmatrix}w_{k-1}, \tag{35}$$

$$y_k = \begin{bmatrix}-2 & 1\end{bmatrix}x_k + 0.2v_k, \tag{36}$$

with $|\zeta_{k-1}| \leq 1$, $w_{k-1} \in W_{k-1} \subset \mathbb{R}$, $v_k \in V_k \subset \mathbb{R}$. Moreover, the initial state $x_0$ satisfies $x_0 \in X_0$.

The system is simulated with $x_0 = \begin{bmatrix}0 & 0\end{bmatrix}^{\mathrm{T}}$, the Gaussian noise realizations are generated by white, uncorrelated and mean normalized GRVs $\mathcal{N}(0,1)$, and $\zeta_{k-1}$ takes values under the uniform PDF in the borders $[-1;1]$.

In order to compare the performance of the KF and the ZF, the state estimation is realized on six different scenarios, namely: (i) reference, (ii)-(vi) poorly tuned. In scenario (i), the parameters of the KF are set as $\hat{x}_0 = \begin{bmatrix}0.5 & 0.5\end{bmatrix}^{\mathrm{T}}$, $P_0^{\mathrm{xx}} = I_{2\times 2}$, $Q_{k-1} = R_k = 1$ and $\zeta_k = 0$, which is its mean. The parameters of the ZF are set as the boxes $\mathcal{X}_0 = \hat{x}_0 \oplus 3I_{2\times 2}[\Phi]^2$, $\mathcal{W}_{k-1} = \mathcal{V}_k = 0 \oplus 3[\Phi]$ and the order reduction $\varphi = 14$, such that each box represents the minimal interval that contain the corresponding noise term with confidence level 99.73%. Moreover, $\mathcal{X}^{\zeta}_{k-1} = 0 \oplus 1[\Phi]$ is a box that represents all possible values of $\zeta_{k-1}$.

In scenarios (ii)-(iv), the tuning of the standard deviation of initial states $\sigma_x$, process noise $\sigma_w$ and measurement noise $\sigma_v$ is increased 100 times, that is, $100\sigma_x$, $100\sigma_w$ and $100\sigma_v$ respectively. In scenarios (v)-(vi), the tuning of the standard deviation of process noise and measurement noise is reduced 100 times, that is, $0.01\sigma_w$ and $0.01\sigma_v$ respectively.

The estimated means and centers are compared through the *root-mean-square error* of the $j$-th state ($\mathrm{RMSE}_j$)

$$\mathrm{RMSE}_j = \frac{1}{100}\sum_{m=1}^{100}\sqrt{\frac{1}{N}\sum_{k=1}^{N}\left(x_{j,k} - \hat{x}_{j,k,m}\right)^2}, \tag{37}$$

where $j = 1,...,n$, is the $j$-th element of the state vector, $N$ is the final time step, and $m$ is the $m$-th Monte Carlo realization.

Moreover, the mean processing time of CPU ($T^{\mathrm{CPU}}$) is used to compare the algorithms. The used computer configuration is: HD 160Gb, RAM memory 3.25Gb, Windows 7 Ultimate, Intel core 2 Quad CPU Q6700 2.66GHz and off-board video card Geforce 9600Gt 512Mb.

### 5.2 State Estimation

Simulated results of KF, ZF with segment minimization ($\mathrm{ZF}_{\mathrm{min.seg}}$) and volume minimization ($\mathrm{ZF}_{\mathrm{min.vol}}$) are presented in Figures 2-4 for one Monte Carlo realization. For the zonotope algorithms, $\mathrm{ZF}_{\mathrm{min.seg}}$ and $\mathrm{ZF}_{\mathrm{min.vol}}$, the order reduction $\varphi$ is such that similar results are obtained using $\varphi > 14$. In Figure 2, where the tuning for each filter is the reference, the usual confidence level $3\sigma_x$ (99.73%) of the KF is more accurate than the interval $\triangle\{\mathcal{X}_k\}$ of ZFs due to the PDF of noise terms being known exactly.

In Table 1, the mean and center estimates for scenario (i) are compared after 100 Monte Carlo realizations. As this scenario consists of exactly known Gaussian uncertainties, the KF is optimal. Therefore, the estimated means are more accurate than the estimated centers. As the segment approach minimizes the Frobenius norm, its centers are more accurate than the volume approach. The index $T^{\mathrm{CPU}}$ for KF, $\mathrm{ZF}_{\mathrm{min.seg}}$ and $\mathrm{ZF}_{\mathrm{min.vol}}$ is 0.069ms, 3.92ms and 20.1ms, respectively. The index $T^{\mathrm{CPU}}$ for ZFs is the largest due to the zonotope order increasing over time. Furthermore, the segment minimization is much faster than the volume minimization, since this last approach generates one more time candidate zonotope and computes its volume, in order to choose that with the smallest volume.

(a)

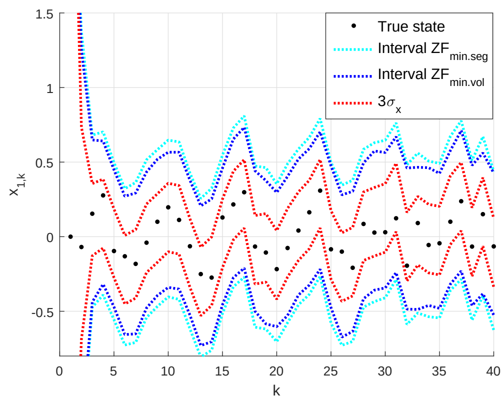


(b)

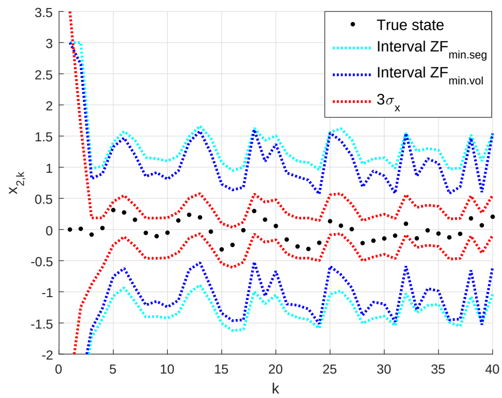


Figure 2: State estimation of the linear system for the scenario (i), reference. (a) and (b) present results of the true states in black points, the confidence level $3\sigma_x$ for the KF in red dotted lines, such that $\sigma_{x_{i,k}} \triangleq \sqrt{P^{\mathrm{xx}}_{(i,i),k}}$ for $i = 1, 2$, and the interval $\triangle\{\mathcal{X}_k\}$ for the zonotope algorithms in cyan ($\mathrm{ZF}_{\mathrm{min.seg}}$) and blue ($\mathrm{ZF}_{\mathrm{min.vol}}$) dotted lines, for one Monte Carlo realization.

In other scenarios, the index $T^{\mathrm{CPU}}$ does not change in relation to scenario (i). In scenario (ii), the obtained results (not shown) converge to scenario (i) after a few iterations. It occurs in the ZF due to the prediction step being computed exactly. Therefore, KF and ZF are not sensitive to initial conditions for linear cases.

Table 1: RMSE of estimated means and centers with segment minimization ($\mathrm{ZF}_{\mathrm{min.seg}}$) and volume minimization ($\mathrm{ZF}_{\mathrm{min.vol}}$), for scenarios (i), (iii)-(vi) after 100 Monte Carlo realizations.

| | (i) | (iii) | (iv) | (v) | (vi) |
|---|---|---|---|---|---|
| $\hat{x}_1^{\mathrm{KF}}(10^{-2})$ | 7.73 | 67.1 | 15.9 | 14.4 | 8.72 |
| $\hat{x}_1^{\mathrm{ZF}_{\mathrm{min.seg}}}(10^{-2})$ | 7.78 | 8.53 | 12.4 | 10.7 | 7.86 |
| $\hat{x}_1^{\mathrm{ZF}_{\mathrm{min.vol}}}(10^{-2})$ | 8.17 | 8.60 | 14.2 | 8.11 | 8.18 |
| $\hat{x}_2^{\mathrm{KF}}(10^{-2})$ | 11.2 | 134 | 18.2 | 17.0 | 11.7 |
| $\hat{x}_2^{\mathrm{ZF}_{\mathrm{min.seg}}}(10^{-2})$ | 12.6 | 13.3 | 14.4 | 12.9 | 12.9 |
| $\hat{x}_2^{\mathrm{ZF}_{\mathrm{min.vol}}}(10^{-2})$ | 18.8 | 18.6 | 16.7 | 18.4 | 18.6 |

(a)

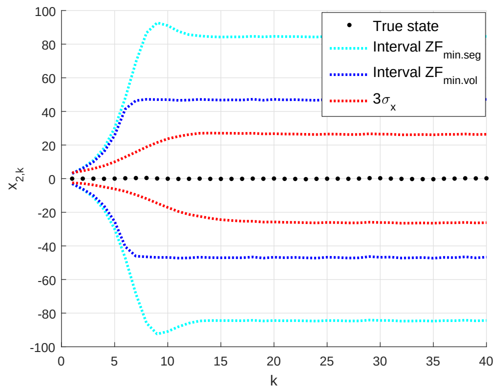


(b)

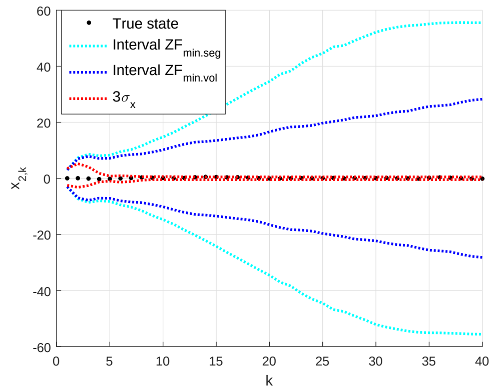


Figure 3: State estimation of the linear system in scenarios (iii), $100\sigma_w$, and (iv), $100\sigma_v$, related to (a) and (b) respectively, for one Monte Carlo realization. Results of the true states in black points, the confidence level $3\sigma_x$ for the KF in red dotted lines and the interval $\triangle\{\mathcal{X}_k\}$ for the zonotope algorithms in cyan ($\mathrm{ZF}_{\mathrm{min.seg}}$) and blue ($\mathrm{ZF}_{\mathrm{min.vol}}$) dotted lines are presented for one Monte Carlo realization.

Figures 3-4 present the state estimation $x_2$ for the scenarios (iii)-(vi). In scenarios (iii) and (v), where only the process noise tuning is modified, the KF demonstrates to be more sensitive than the ZFs, since the *a posteriori* covariance $P_k^{\mathrm{xx}}$ is proportional to a priori covariance $P_{k|k-1}^{\mathrm{xx}}$. On other hand, in scenarios (iv) and (vi), where only the measurement noise tuning is modified, ZFs demonstrate to be more sensitive than the KF, since the width modification of the strip $\mathcal{Y}_{k|k-1}$ influences the intersection $\mathcal{X}_k$ more than the prediction $\mathcal{X}_{k|k-1}$ does. Due to these sensitivities, the KF fails to include the true states in scenario (v) while the intervals of the ZFs does not, since they are more conservative.

(a)

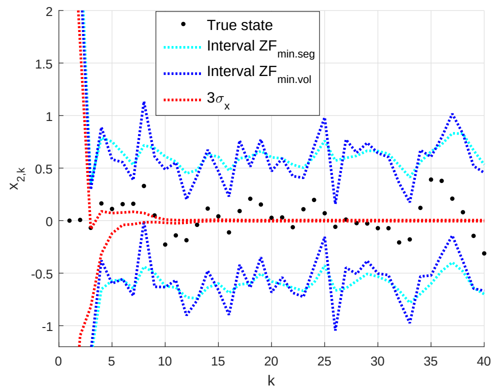


(b)

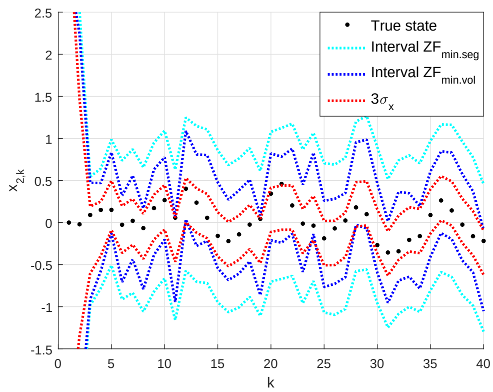


Figure 4: State estimation of the linear system in scenarios (v), $0.01\sigma_w$, and (vi), $0.01\sigma_v$, related to (a) and (b) respectively, for one Monte Carlo realization. Results of the true states in black points, the confidence level $3\sigma_x$ for the KF in red dotted lines and the interval $\triangle\{\mathcal{X}_k\}$ for the zonotope algorithms in cyan ($\mathrm{ZF}_{\mathrm{min.seg}}$) and blue ($\mathrm{ZF}_{\mathrm{min.vol}}$) dotted lines are presented for one Monte Carlo realization.

## 6 Conclusions

This paper presented a comparative analysis between two methods to estimate states of a given uncertain linear system, namely: stochastic approach, represented by the KF, and zonotopic approach, represented by the ZF. According to the KF, the *a posteriori* mean and covariance seek to characterize the true states by means of a Gaussian PDF. This algorithm provides an analytically closed solution and a region to include the true states, which is represented by a quantity of the standard deviation. Since the noise terms are well represented by GRVs, accurate results are generated around the true states. On other hand, the ZF works on the set membership approach to characterize uncertainties. This method is called guaranteed estimation, since the true states are included into the estimated sets under the design hypothesis. In order to achieve that, it is necessary to guarantee that initial states and noise terms are included into their sets, which are deterministically chosen. Thus, set membership estimators work on the worst case of noise, leading to more conservative results at the same time. This filter is not optimal and it provides an approximated numerical solution, since the data-assimilation step is overestimated. The ZF can be used with the segment minimization or volume minimization approaches. The first one is the fastest while the second one is the most accurate. Although processing time of the volume minimization has been improved in (Bravo et al., 2006), the zonotope order increase can lead the ZF to be much slow. This is the main reason to apply an order reduction on zonotopes, but it leads to more conservative sets, which can become so large when the order is close to the dimension of the Euclidean space. By means of numerical results, the sensitivity to noise tuning of both KF and ZF was made explicit. In general, when the tuning is accurate, the KF highlights due to its optimality. In other tuning cases, the ZF calculates more accurate centers with larger uncertainty. Moreover, the segment minimization generates better center than the volume minimization, due to the Frobenius norm being related to the 2-norm.

## Acknowledgments

This work has been supported by the Brazilian agencies CAPES, FAPEMIG and CNPq.

## References

Alamo, T., Bravo, J. M. and Camacho, E. F. (2005). Guaranteed state estimation by Zonotopes, *Automatica* **41**(6): 1035–1043.

Bravo, J. M., Alamo, T. and Camacho, E. F. (2006). Bounded error identification of systems with time-varying parameters, *IEEE Transactions on Automatic Control* **51**(7): 1144–1150.

Combastel, C. (2005). A state bounding observer for uncertain non-linear continuous-time systems based on zonotopes, *Proceedings of the 44th IEEE Conference on Decision and Control*, pp. 7228–7234.

de Almeida Neto, M. M., Schreiber, L. and Raffo, G. V. (2014). Robust state estimation for UAVS - a comparison study among a deterministic and a stochastic approach, *XX Congresso Brasileiro de Automática, 2014, Belo Horizonte*, Anais do XX Congresso Brasileiro de Automática, pp. 3429–3436.

Gelb, A. (1974). *Applied optimal estimation*, MIT press.

Jazwinski, A. H. (2007). *Stochastic processes and filtering theory*, Courier Corporation.

Kalman, R. E. et al. (1960). A new approach to linear filtering and prediction problems, *Journal of basic Engineering* **82**(1): 35–45.

Kay, S. M. (1993). *Fundamentals of statistical signal processing*, Prentice Hall PTR.

Le, V. T. H., Stoica, C., Alamo, T., Camacho, E. F. and Dumur, D. (2013). *Zonotopes: From guaranteed state-estimation to control*, John Wiley & Sons.

Moore, R. E., Kearfott, R. B. and Cloud, M. J. (2009). *Introduction to interval analysis*, SIAM.

Rego, B. S. and Raffo, G. V. (2016). Suspended load path tracking control based on zonotopic state estimation using a tilt-rotor UAV, *Intelligent Transportation Systems (ITSC), 2016 IEEE 19th International Conference on*, IEEE, pp. 1445–1451.